Evolution in the Clustering of Galaxies for $Z < 1$

Robert J. Brunner

Department of Astronomy, The California Institute of Technology, Pasadena, CA 91125

Andrew J. Connolly

Department of Physics and Astronomy, University of Pittsburgh, Pittsburgh, PA, 15260

Alex S. Szalay

Department of Physics and Astronomy, The Johns Hopkins University, Baltimore, MD 21218

Abstract.

Measuring the evolution in the clustering of galaxies over a large redshift range is a challenging problem. For a two-dimensional galaxy catalog, however, we can measure the galaxy-galaxy angular correlation function which provides information on the density distribution of galaxies. By utilizing photometric redshifts, we can measure the angular correlation function in redshift shells (Brunner 1997, Connolly *et al.* 1998) which minimizes the galaxy projection effect, and allows for a measurement of the evolution in the correlation strength with redshift. In this proceedings, we present some preliminary results which extend our previous work using more accurate photometric redshifts, and also incorporate absolute magnitudes, so that we can measure the evolution of clustering with either redshift or intrinsic luminosity.

1. Data

The photometric data used in this analysis are located in the intersection between the *HST* 5096 field and the CFRS 14 hour field (*i.e.* the Groth Strip), covering approximately 0.054 Sq. Degree. All of the photometric data were obtained over several observing runs using the Prime Focus CCD (PFCCD) camera on the Mayall 4 meter telescope at Kitt Peak National Observatory (KPNO). All observations were made through the broadband filters $U, B, R, \& I$.

The photometric data were reduced in the standard fashion which is detailed elsewhere (Brunner 1997). Source detection and photometry were performed using SExtractor, which was chosen for its ability to detect objects in one image and analyze the corresponding pixels in a separate image. When applied uniformly to multi-band data, this process generates a matched aperture dataset.

Our detection image was constructed from the $U, B, R, \& \ I$ images using a χ^2 process (Szalay *et al.* 1998).

2. Empirical Photometric Redshifts

The photometric redshifts used in this analysis were derived empirically using a piecewise approximation approach (Brunner *et al.* 1999). Briefly, this approach defines five different redshift intervals which track the movement of the 4000 Å break through our filter system with increasing redshift (for $z < 1.2$). 190 calibrating redshifts were used to derive a global third order polynomial in $U, B, R, \& \ I$ which provided an initial redshift estimate, from which the appropriate local redshift estimate was selected. The range of calibrating redshifts for each polynomial fit was extended by approximately 0.05 in order to diminish end-aliasing effects. This algorithm is designed to generate an optimal redshift for objects by using the more accurate local relations (Brunner *et al.* 1997). For each derived polynomial fit, the degrees of freedom remained a substantial fraction of the original data (a second order fit in four variables requires 15 parameters while a third order fit in four variables requires 35 parameters).

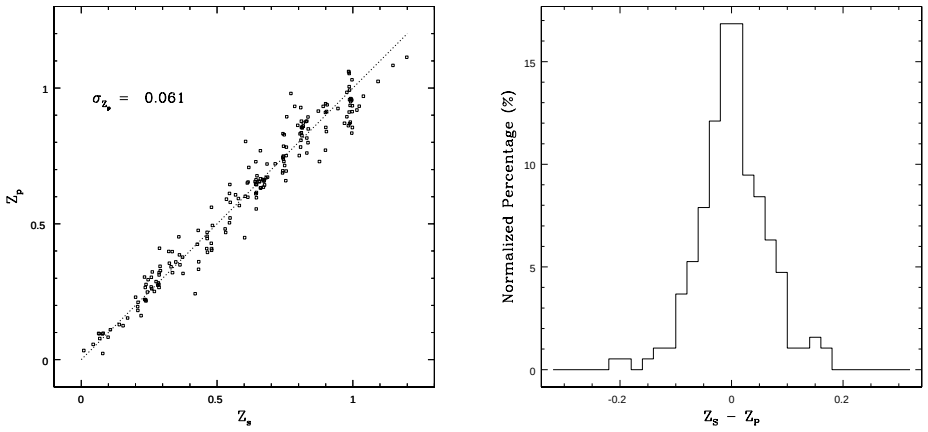

Figure 1. The left hand figure provides comparison between the calibrating spectroscopic redshifts and the estimated photometric redshifts used in this analysis. The intrinsic dispersion in the relationship is $\sigma = 0.061$. The right hand figure provides a histogram view of the residual differences between the spectroscopic and photometric redshifts.

A subtle, and often overlooked, effect in any photometric redshift analysis is the requirement for accurate multi-band photometry. Ideally we could restrict our photometric-redshift catalog to only those objects which have measured magnitude errors below some set limits (*e.g.,* 10% photometry). This type of a restriction, however, introduces two complications: a bias towards blue spectral types, and a subsequently complicated selection effect.

In an attempt to overcome these biases, we restrict the full sample to those objects which have both $I_{AB} < 24.0$ and measured magnitude errors < 0.25

in $U, B, \& R$. This minimizes any selection bias to only faint early-type galaxies. The remaining filter combinations contribute to the noise in our analysis (*i.e.* when we consider our final catalog complete to $I \approx 24.0$), and amount to only a few percent when combined. After removing stars and sources with bad detection flags, our final photometric-redshift catalog contains 3052 sources.

3. Ensemble Approach

A formal, analytic technique is not always available to utilize photometric redshifts and their associated errors when measuring cosmologically interesting quantities. As a result, we have developed an alternative technique, the galaxy ensemble approach. Essentially, we treat the problem in the context of statistical mechanics, where each galaxy is localized in redshift space by a Gaussian probability distribution function. To calculate a physically meaningful quantity, we create multiple realizations (or ensembles) of the galaxy redshift distribution, and calculate the appropriate quantity for all of the different ensembles. We then average the different measurements to produce the desired value, simultaneously producing a realistic error estimate. This can easily be done for the redshift distribution of the galaxy sample, where an analytic approach is also available for comparison (*cf.* Brunner *et al.* 1999).

This approach was used to generate absolute magnitude distributions in both the U and B bands for this data. First, a set of 100 redshifts were estimated for each source by drawing redshifts randomly from a Gaussian probability distribution function (PDF) with mean and sigma given by the calculated photometric redshift and photometric redshift error. For each redshift in the ensemble, a k-correction was calculated using the assigned spectral type. Apparent magnitudes were estimated for every source in the ensemble by drawing them from a Gaussian PDF with mean and sigma given by the measured magnitude and magnitude error. Using the k-corrections, apparent magnitudes, and an assumed cosmology, 100 different absolute magnitude distributions in both B and U were generated.

4. Angular Correlation Function

Before computing the angular correlation function, we determined the regions within our image in which the detection efficiency might be reduced. The primary areas where this occurs are around bright stars, in charge transfer trails, and near the edge of the frame due to edge effects or focus degradations. We, therefore, defined bounding boxes, for each of the four stacked images, which contained all of the observable flux for the saturated stars within the image. These four mask files were concatenated to produce a total mask file which was used for the calculation of the angular correlation function in different redshift intervals.

We used the optimal estimator $(DD - 2DR + RR)/RR$ (Landy & Szalay 1993), where D stands for data and R stands for random, to determine the angular correlation function. This required counting the number of observed pairs (that were not within the masked areas), which was done in 10 bins of constant width $\Delta \lg(\theta) = 0.25$, centered at $\theta = 4.3''$, to $\theta = 759.6''$. 1000 objects

were then randomly placed in the non masked areas within the image, and the data-random and random-random correlation functions were calculated for the same angular bins used for the data-data auto-correlation function.

This estimator uses the calculated number density of galaxies within the CCD frame to estimate the true mean density of galaxies. The small angular area of our images introduces a bias in the estimate, commonly referred to as the "Integral Constraint" (Peebles 1980). We estimated a correction for this bias following the prescription of Landy and Szalay (1993), which is subtracted from the $(DD - 2DR + RR)/RR$ value.

The error in the estimation of the angular correlation function is assumed Poisson in nature, and is calculated as the square root of the number of random-random pairs in each angular bin.

5. Evolution in the Clustering of Galaxies

The multivariate angular correlation function $w(\theta, z_P)$ was determined for nine different redshifts by binning the data in redshift bins of width $\Delta z_P = 0.2$ centered at $z_P = 0.2$ to $z_P = 1.0$. The nine different functions are calculated for the 258, 330, 327, 420, 640, 715, 713, 732, and 514 objects in the different respective redshift bins. For each redshift region, a least squares fit was performed assuming the relation $w(\theta) = A_w \theta^{-0.8}$. The amplitude was then measured by minimizing the absolute deviation with respect to A_w, which in this case reduces to finding the median of the measured correlation function amplitudes.

Previously, two methods have been used to quantify the evolution in the clustering of galaxies. The first technique is to invert the angular correlation function $(w(\theta))$ using the Limber equation (Peebles 1980) and an observed or model redshift distribution to estimate the expected change in the amplitude of the angular correlation function for different magnitude intervals and/or cosmologies. The other approach is to compute the spatial correlation function $(\xi(r))$ for different epochs directly using spectroscopic redshifts. These two techniques, however, suffer from different limitations that have restricted their utility.

Studies which utilize different magnitude intervals are limited by the redshift smoothing effects of an apparent magnitude limited sample, much the same as the number magnitude distributions. The spectroscopic approach is hindered either by the size of the available samples, especially when the data is binned into distinct redshift intervals, or by the depth of the survey. These studies are also affected (up to a factor of two) by the redshift space distortions due to density inhomogeneities.

We adopt the novel approach of computing the amplitude of the multivariate angular correlation function for the 3052 objects in the photometric redshift–template SED catalog in redshift bins of width $\Delta z = 0.2$. To compare these observations to semi-analytic theory, we assume a power law model for the spatial clustering (Peebles 1980),

$$\xi(r, z) = \left(\frac{r}{r_0}\right)^{-\gamma} (1 + z)^{-(3+\epsilon)}$$

where $\gamma \approx 1.8$ and $r_0 \approx 3.0\ h^{-1}$ Mpc in co-moving coordinates as measured locally. The three canonical values of the evolution (assuming $\gamma = 1.8$) are $\epsilon = 0.8$ as predicted by linear theory, $\epsilon = 0.0$ for clustering fixed in proper coordinates, and $\epsilon = -1.2$ for clustering fixed in co-moving coordinates. The change in A_w with redshift is displayed in Figure 2 along with the three different evolution models for $\Omega = 1.0$ and $\Omega = 0.1$. The error in A_w was calculated by estimating A_w in each redshift interval for the 1σ upper and lower values.

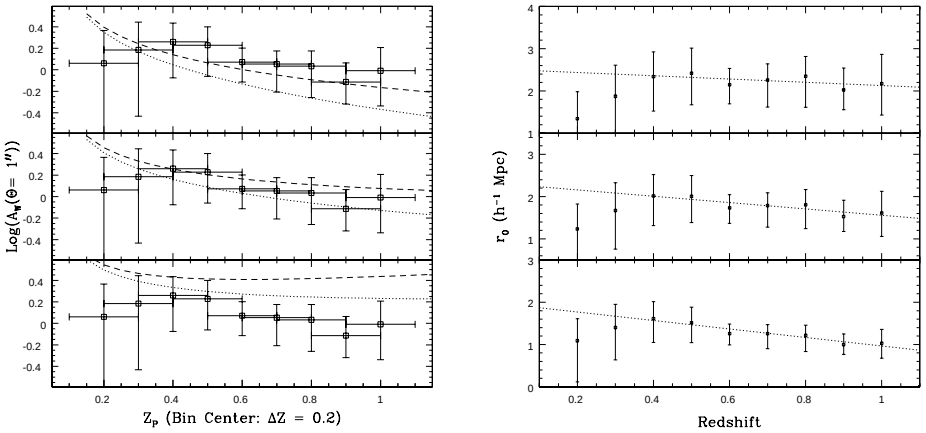

Figure 2. The left hand figure displays the evolution in the amplitude of the angular correlation function with redshift. The three lines are predictions for $\Omega = 0.1$ (dotted line) and $\Omega = 1.0$ (dashed line) using Limber's equation. The right hand figure shows the evolution in the correlation length (r_0) with redshift assuming $\Omega = 1.0$ using Limber's equation and the redshift distribution measured from the galaxy redshift ensemble. In each figure, the top panel assumes the evolution parameter derived from linear theory ($\epsilon = 0.8$), the middle panel assumes fixed clustering in proper coordinates ($\epsilon = 0.0$), and the bottom panel assumes fixed clustering in co-moving coordinates ($\epsilon = -1.2$).

Of the three different scenarios, the predictions for clustering fixed in co-moving coordinates ($\epsilon = -1.2$) are the least consistent with our data, independent of the value of Ω. The predictions of linear theory ($\epsilon = 0.8$) are mildly consistent for high values of Ω, while the best agreement is for clustering fixed in proper coordinates ($\epsilon = 0.0$), independent of the value of Ω. Our technique is less sensitive to redshift distortions than the spatial correlation approach due to the width of our redshift bins. Furthermore, our technique does not require model predictions for the redshift distribution of galaxies as does the apparent magnitude interval approach.

The novel measurement of the evolution in the clustering of galaxies with absolute magnitude we have presented in Figure 3 is consistent with both the general expectation of most structure formation theories and similar low redshift observations. Further improvements in this technique are forthcoming (Brunner *et al.* 1999b), and will include measurements of the evolution of the correlation length with both redshift and absolute magnitude, as well as a conversion from

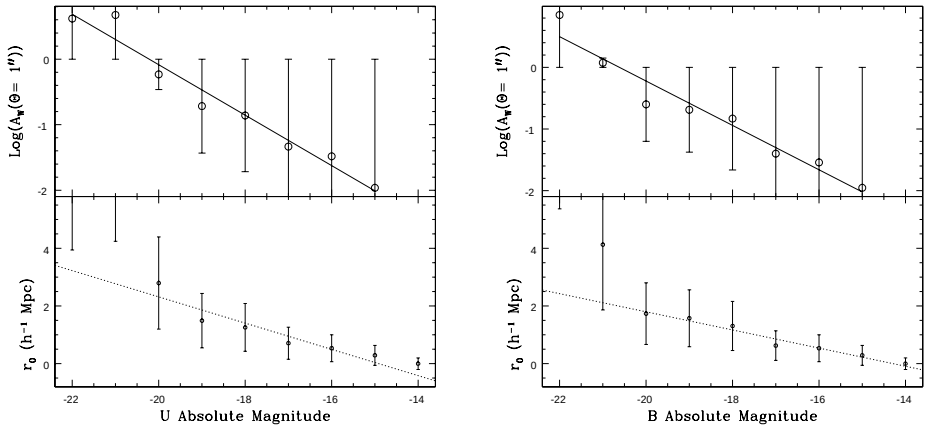

Figure 3. These two panels show the evolution of the amplitude of the angular correlation function with absolute magnitude (top) and the evolution of the correlation length with absolute magnitude (bottom) for the U (right) and B (left) bands. No segregation by redshift was used in this analysis. The absolute magnitudes are generated using the 100 different realizations with the ensemble approach. The amplitude of the correlation function was converted to R_0 using Limber's equation with $\Omega = 1$ and $\epsilon = 0.0$ and integrating over entire redshift range.

the amplitude of the correlation function (A_w) to the correlation length (r_0) in a model (*i.e.* ϵ) free technique.

Acknowledgments. We wish to thank George Djorgovski, Mark SubbaRao, Gyula Szokoly, and Lori Lubin for useful Discussion. AJC acknowledges partial support from HST (GO-07817-02-96A) and LTSA (NRA-98-03-LTSA-039), AS from NASA LTSA (NAG53503), HST Grant (GO-07817-04-96A).

References

Brunner, R.J, PhD. Thesis, The Johns Hopkins University, 1997.

Brunner, R.J, Connolly, A.J., Szalay, A.S., & Bershady, M.A., 1997, ApJ, 482, L21.

Brunner, R.J, Connolly, A.J., & Szalay, A.S., 1999, ApJ, 516, 563.

Brunner, R.J, *et al.*, 1999b, in preparation.

Connolly, A.J., Csabai, I., Szalay, A.S., Koo, D.C., Kron, R.G., and Munn, J.A., 1995, AJ, 110, 6.

Connolly, A.J., Szalay, A.S., & Brunner, R.J., 1998, ApJ, 499, L125.

Landy, S.J., & Szalay, A.S., 1993, ApJ, 412, 64.

Peebles, P.J.E., 1980, *The Large Scale Structure of the Universe.*, Princeton University Press.

Szalay, A.S., Connolly, A.J., & Szokoly, G.P., 1998, submitted.